

Relation of the String Tension Among Quarks with Various Distinctive Features of QCD

Navjot Hothi* and Shuchi Bisht†

Department of Physics, Kumaun University, Nainital-263002, Uttarakhand, India

Received 4 February 2012, Accepted 10 August 2012, Published 15 January 2013

Abstract: The string tension is a characteristic quantity in discussing confinement physics and we have investigated the relation and impact of string tension upon various distinctive features of Quantum-Chromodynamics (QCD). These include the behavioural implications of string tension corresponding to varying temperatures under different QCD phases. Also, the string tensions in the large N_c limit are interrogated and effort is made to determine the proximity of $N_c = 3$ limit with the large N_c limit. We have tried to study the effective spatial string tension in quenched $SU(N_c)$ QCD under the gluon chain model when temperatures are considered below the critical deconfinement temperature. The spatial string tension is also visualized within a five dimensional AdS/QCD framework. Furthermore, we determined the implications of the string tension parameter upon the glueball dynamics. The $N_c = 3$ and $N_c = 2$ limits display evident intimacy and they extensively stand apart from the $N_c = 1$ limit. Clear intrinsic connection is visible between $N_c = 3$ and $N_c = \infty$ limit. Furthermore, the spectrum of hybrid particles and gluelumps is found to be implicitly dependent upon the string tension and experimental data can be reproduced within this framework. An intrinsic relation is sought between the Regge trajectory phenomenology and the string tension between quarks.

© Electronic Journal of Theoretical Physics. All rights reserved.

Keywords: Spatial String Tension; Wilson Loops; K-Strings; Scaling; Regge Trajectories

PACS (2010): 12.38.-t; 11.25.Wx; 12.38.Gc; 12.39.Mk; 11.55.Jy

1. Introduction

One of the most prominent features of QCD is quark confinement [1,2]. Quark confinement is now an old and familiar idea, but familiarity does not imply understanding. No theory of quark confinement is generally accepted and every proposal is controversial. Nevertheless, there have been given some very interesting explanations of this phenom-

* Email: hothi.navjot@gmail.com

† Email: shbisht@gmail.com

ena, most of which share the feature that topological excitations of the vacuum play a major role. These pictures include among others, the dual superconductor picture of confinement [3,4]. This picture of confinement is based upon the analogy between the superconductor and the QCD vacuum [5]. Stringlike chromoelectric flux tube is formed between distant static quarks. This leads to their confinement, with an energy proportional to the distance between them and also leads to the vanishing of the colour dielectric constant. Thereby, QCD witnesses the inclusion of 'stringlike' degrees of freedom called QCD strings or QCD flux tubes. These stringlike excitations are responsible for the confinement of colour charges since the charges are always attached to at least a string. These strings have tension and the energy per unit length defines the string tension. Thus, this picture portrays a framework within which the quarks are tied together by strings. Numerical simulations of QCD, that is lattice QCD [6] successfully demonstrates the validity of this conjecture. We have demonstrated the dependency and implications of the string tension parameter upon various distinctive features of QCD and have tried to analyze this parameter through all possible aspects.

We have studied the thermodynamics of QCD, both below and above the deconfinement temperature. The interest in QCD at temperatures larger than a few hundred MeV is triggered not only by pure theoretical reasons, but also by ongoing heavy-ion collision experiments and by cosmology. These heavy ion collisions aim at creating quark-gluon plasma in the laboratory. Recent RHIC experiments [7,8] suggest that the quark-gluon plasma may be more than a perfect liquid and spatial string tensions prevail in this high temperature regime. The spatial string tension can be easily extracted as the coefficient in the area law of large rectangular Wilson loops [9]. Spatial string tension is also important to verify the theoretical concept of dimensional reduction at high temperatures [10]. The spatial string tension serves as a classic non-perturbative probe for the convergence of the weak coupling expansion at high temperatures.

The spatial string tension can be studied within a number of frameworks such as the gluon chain model [11], where quenched $SU(N_c)$ QCD approximations are utilized. Here, the spatial string tension behaviour is exclusively studied for temperatures less than the critical temperature and visible behavioural differences between the $N_c=1$ and $N_c=3$ limits are projected out. For temperatures greater than the critical temperature, we have studied the spatial string tension within a five dimensional framework, known as AdS/QCD [12]. We observed that the temperature dependence of string tension is very soft below T_c and sharp above T_c .

Furthermore, we also tried to determine the affect of scaling upon confinement. Real confinement actually corresponds to intermediate distances and not the large distance scales, for then the electric flux tubes would break and the static potential would go flat. For intermediate distances, a linear potential is obtained and the string tensions for this regime obey scaling laws namely the Casimir scaling [13] and the sine scaling [14] (flux tube counting). The string tensions agree qualitatively with both the Casimir scaling and the flux tube counting. It is however worth noting that the $N_c=3$ limit is quite close to $N_c=\infty$ limit and the QCD theory becomes exceedingly simple if these two limits show

proximity to each other. However, it worth noting that for $N_c > 3$, new strings come into existence, which are also confining [15]. These strings are called k-strings. The ratio of k string tension to the fundamental string tension can be studied under Casimir scaling as well as the sine scaling[16]. The sine scaling is supposed to coincide with Casimir scaling in the large N limit. Our analysis also favours this particular conjecture.

Next, we have also tried to explore the domain of glueball dynamics with the string tension parameter. The glueball dynamics is inherently dependent upon the the adjoint string model and a close scrutiny of the formalism developed under this approach reveals that the adjoint string tension is directly dependent upon N_c . The propagation of gluon in the confining vacuum is studied within the framework of the Background Perturbation Theory (BPT)[17], where non perturbative backgrounds contain confining co-relaters. This procedural approach helps in determining an intrinsic connection between the mass of hybrid particles and gluelumps with the string tension parameter. The mass of the hybrid particles is dependent upon two variable parameters, namely the string tension and the separation, whereas the mass of the gluelump depends upon the string tension parameter alone as the separation approaches zero for the gluelump limit. We evaluated the hybrid masses and have co-related our data to the experimental front. The string tensions for the gluelump spectra have also been evaluated.

The earliest visualizations of the numerical value of string tensions came from the Regge trajectory phenomenology. The Chew-Frautschi conjecture[18] stated that the strongly interacting particles (hadrons) are self generating and must lie on straight lines. Scarcity of hadronic data led to the postulation that slopes of hadronic RTs is constant and thereby the QCD strings within these hadrons possess constant value of string tension. This hypothesis witnessed an eventual violation. The true imprints of the hadronic world are portrayed by the hadronic data itself. We utilized the latest hadronic data[19] available through the Particle Data Group[20] and evaluated string tensions for both mesonic as well as baryonic RTs which are either the essentially linear or fairly linear or even essentially non-linear.

2. Role of Spatial String Tension in QCD Thermodynamics

A broad spectrum of research areas such as Cosmology, Astrophysics and Heavy-Ion-Phenomenology are implicitly dependent upon the calculation of QCD thermodynamics from the first principle. Recently, lattice QCD [21] has proven to be the richest source to perform such calculations. The study of QCD at temperatures larger than (a few) hundred MeV helps in probing the property of asymptotic freedom. Thus, the study of the weak coupling expansion of this high temperature phase becomes viable. The spatial string tension thereby projects out as a classic non-perturbative probe for the convergence of weak coupling expansion at high temperatures. However, we are well aware of the fact that at the confinement temperature T_c , the physical string tension becomes zero.

The calculation of spatial string tension is important to verify the theoretical concept of dimensional reduction at high temperatures[10]. The spatial string tension is

extracted from the spatial static quark potential of the spatial Wilson loops[22]. The Wilson loop serves as an important tool for studying confinement in gauge theories. The gauge string/duality is itself useful to calculate the Wilson loop from string configurations[9]. Using a simple argument on the behaviour of horizontal Wilson loops at high temperature, a general relation between deconfinement point T_c and string tension can be obtained.

It was understood however that in non-Abelian gauge theories the Wilson loop for large space like contours obeys the area law at arbitrary temperature [22]. This phenomenon is known as magnetic confinement and yields non-zero string tension. This can be dynamically understood by the fact that when the temperature of the system is increased, there is reduction in the phase space of the colour flux tube until it fills the whole space. Now, the flux tube begins to be squeezed between the two opposite sides of the temporal box. At temperatures far above the deconfinement temperature, the distribution of the colour flux tube along the temporal axis becomes uniform. Thus, the translational invariance in the time direction is restored and the Goldstone field describing the field fluctuations disappear. Even when the deconfinement phase transition was investigated by numerical simulations on lattice for pure SU(3) gauge theory[23], the data demonstrated strong suppression of the electric component of the correlator above T_c and subsequent persistence of the magnetic component. The contribution of the magnetic correlator remains visible even across the phase transition temperature. On the contrary, the electric part suddenly vanishes above T_c making the electric condensate drop to zero at the deconfining phase transition point [24]. Mathematically, the spatial string tension can be expressed as the coefficient in the area law of a large rectangular Wilson loop $W_s(R_1, R_2)$ in the (x_1, x_2) plane and can be expressed as [25]:-

$$\sigma_s = -\lim_{R \rightarrow \infty} \lim_{R \rightarrow \infty} \frac{1}{R_1 R_2} \ln W_s(R_1, R_2) \quad (1)$$

Lattice simulations [26] indicated that at $T \geq 2T_c$, the magnetic fields as determined by spatial string tension starts growing quadratically as $\sigma_s(T) \sim T^2$ which projects forth the advent of a new visualization, called the dimensional reduction. Under this particular framework, the temporal direction is squeezed and the higher Matsubara frequencies are suppressed. This leads to the effective reduction of dynamics to three dimensional gluodynamics [27]. Thus, three dimensional lattice calculations help in the determination of physical quantities such as $\sigma_s(T)$. We have studied the spatial string tension under two different models, which portray its behaviour both above and below the deconfinement temperature.

3. Effective Spatial String Tension in Quenched SU(N_c) QCD under the Gluon Chain Model

String dynamics itself help in determining the deconfinement critical temperature T_c . When the string connecting heavy quark-antiquark pair passes through heavy valence

gluons (forming a gluon chain), very high entropy is generated in this system. It provides a viable mechanism for predicting the value of T_c and also helps in studying the critical behaviour of string tension below T_c [11]. In this particular section, we have portrayed the effective distinction between the $N_c=3$ and $N_c=1$ limit using the parameterisation of the gluon chain model.

Soft stochastic background gluonic fields lead to the production of quark-antiquark strings, which sweeps out the flat surface of the corresponding Wilson loop. Moreover, string vibrations are produced by the fluctuations of the gauge field. These fluctuations could be related to the valence gluons through which the quark-antiquark string passes. The string may pass through many valence gluons leading to the production of the gluon chain. The energy of a single string bit between two nearest gluons in a chain is constant. It is worth noting that as long as thermal mass of a valence gluon is smaller (at low temperatures) than this energy, the general global dynamics of the string is unaffected and the gluons move together with the string. Further, when the system is heated, and at a certain temperature T_0 , the gluons thermal mass ($\propto T$) becomes larger than the free energy of the string bit. Now, there is a drastic change in the configuration of the system and the gluons become nearly static from the strings standpoint. Thereby, at temperatures, T , such that $T_0 < T < T_c$, the gluons chain behaves as a sequence of static nodes with adjoint charges linked by independently fluctuating string bits. It is here that the entropy of the system becomes large. This occurs due to the fact that the gluon chain originating from a quark randomly walks over the lattice of static nodes towards an antiquark. The entropy of the system increases due to the fact that colour may change from one node to another during this random walk. This implies that every string bit may transport each of the N_c colour. This increase in the entropy of the system leads to the deconfinement phase transition.

The total free energy of the system is the sum of the usual linear potential and the free energy of the random walk. The entire procedural approach starts with the calculation of partition function for the gluon chain and the effective string tension, which is dependent upon the partition function is given as

$$\sigma(T) = \sigma - T \ln \frac{Z(R, T)}{Z_0(R, T_0)} \Big|_{R \rightarrow \infty} \quad (2)$$

where $Z(R, T)$ is the partition function of the random walk and is given by

$$Z(R, T) = \sum_{n=-\infty}^{\infty} \int_0^{\infty} \frac{ds}{(4\pi s)^2} \exp\left[-\frac{R^2 + (\beta n^2)}{4s} - \frac{s}{a}(\beta\sigma - \frac{\ln N_c}{a})\right] \quad (3)$$

Here $s=aL$ is the Schwinger proper time (a is the length of one bit of string and L is the length of the gluon chain), $\beta = 1/T$, σ is the zero temperature string tension and n is the number of a Matsubara mode. The $n=0$ term is significant at asymptotically large R 's, which is basically the region of interest and then

$$\sigma(T) = \sigma + T \left[\sqrt{\frac{\sigma\beta}{a} \left(1 - T \frac{\ln N_c}{\sigma a}\right)} - \sqrt{\frac{\sigma\beta_0}{a} \left(1 - T_0 \frac{\ln N_c}{\sigma a}\right)} \right] \quad (4)$$

The value of T_c is estimated from the condition that the argument of the first square root vanishes and its value comes out to be $T_c = 270$ MeV [28] for $N_c=3$ and the effective length of one string bit is $a \sim 0.31$ fm. T_0 can be evaluated from the formula:

$$T_0 = \frac{T_c}{\ln N_c + 1} \sim 130 \text{ MeV} \quad (5)$$

Now, considering the limiting case, when the string bits cannot change colour, then $N_c=1$ and equation 2 yields

$$\sigma(T) = \sigma + \sqrt{\frac{\sigma T}{a}} \left(1 - \frac{T}{T_0}\right) \quad (6)$$

In this particular case, T_0 can be determined directly from the equality of the gluons thermal mass in QCD to the free energy of one string bit [11],

$$T_0 = \frac{\sigma a}{s} \quad (7)$$

For $a=0.22$ fm and $g=2.5$, giving $T_0 = 85$ MeV and the critical temperature [11] $T_c=290$ MeV. Thus, for temperatures $T_0 < T < T_c$, the spatial string tension behaviour is implicitly dependent upon two prominent features that is the physical string tension and temperature parameter itself. This particular analysis exhibits the fact that spatial string tension variation pattern can be effectively determined by varying these two parameters within their specified range. The physical string tension is varied within a range 0 to 0.2 GeV^2 . We have plotted a three dimensional spreadsheet which clearly helps in visualising the spatial variation. Figures 1 and 2 display the variation pattern for $N_c=1$ and $N_c=3$ respectively. Both the plots display observable differences and provide a platform for demonstrating evident difference between the $N_c=1$ and $N_c=3$ limit. It may however be pointed out that for temperatures far above the critical temperature (more than a few hundred MeV), the spatial string tension displays a linear variation with the temperature. The spreadsheet for $N_c=1$ limit covers the entire available spatial dimensions, whereas the $N_c=3$ three dimensional plot is restricted within a smaller domain and the spreadsheet possesses an effective curvature. Thus, we can conclude by saying that $N_c=3$ formalism stands effectively apart from the $N_c=1$ conjecture.

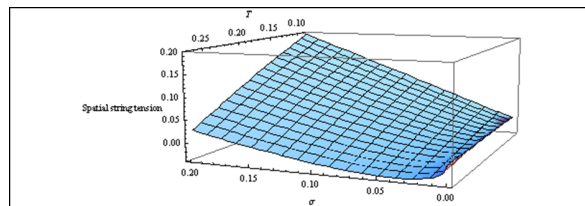


Fig. 1 Spreadsheet displaying the variation of spatial string tension (in GeV^2) with temperature (in MeV) and physical string tension (in GeV^2) for $N_c=1$.

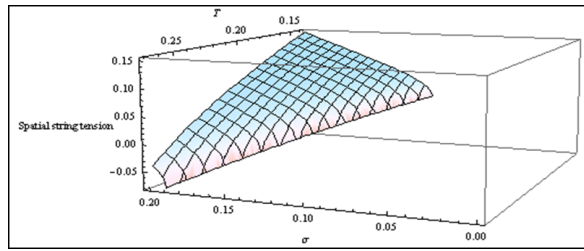


Fig. 2 Spreadsheet displaying the variation of spatial string tension(in GeV^2) with temperature(in MeV) and physical string tension(in GeV^2) for $N_c=3$.

4. Spatial string tension under the AdS/QCD framework

We have scrutinized the modelling of temperature dependence of spatial string tension within a five dimensional framework, known as AdS/QCD[12]. The $SU(N)$ gauge theories undergo a phase transition to a deconfined phase at high temperature. The pseudo-potential extracted from spatial Wilson loops does not exhibit quantitative drastic change at deconfinement temperature T_c . This owes to the fact that certain confining properties survive in the high temperature phase. High temperature perturbation theory is helpful in determining the behaviourism of pseudo potential for temperatures well above T_c . However, near the phase transition point, the non-perturbative effects pose difficulties in the computation of the pseudo potentials. At this point, the AdS/QCD approach came to the rescue which deals with a string description of strong interactions.

The five dimensional AdS/QCD approach helps in exploring the temperature dependence of the spatial string tension. Spatial Wilson loops are studied which obey an area law and provide string tension. The whole framework of this approach relies upon c , which is the Regge parameter at zero temperature and its value ($c \sim 0.9 GeV^2$) is fixed from the ρ meson Regge trajectory[29], with the co-efficient of proportionality fixed from the linear term of the Cornell potential.

A rectangular loop C is considered along two spatial directions (x,y) on the boundary($z=0$) of a five dimensional space. One of the direction is taken to be large, say $Y \rightarrow \infty$ and the quark and antiquark are positioned at $x=r/2$ and $x=-r/2$ respectively. The Nambu-Goto action with the world sheet co-ordinates x and y is evaluated and equation of motion for z is determined. The z dependent effective string tension as followed from the AdS metric is viewed simply as

$$\sigma(z) = z^{-2} \exp\left[\frac{1}{2}cz^2\right] \quad (8)$$

The behaviour of potential $V=\sigma(z)$ shows that it reaches a minimum value at $z=z_c$ ($z_c = \sqrt{\frac{2}{c}}$ and $z_0 = z$, when $x=0$), where the repulsive force prevents the string from getting deeper in the z direction. Because the string ends on infinitely heavy quark antiquark pair set at $z=0$, it faces a minima of potential which can be termed as a wall with condition

$$z_o < z_c \quad (9)$$

Also, in the limit as c goes to 0, z_0 is bounded by a horizon ($z=z_T$) and this gives rise

to a wall

$$z_0 < z_T \quad (10)$$

Thus, two walls become pertinent in this visualization. This projects out to be the most prominent factor in determining the temperature dependence of the spatial string tension.

Temperature dependence of spatial string tension is determined by evaluating r , which is a continuously growing function of z_0 . This means that large distances correspond to a region near the upper endpoint which is the smallest of z_c and z_T and this leads to $v \sim 1$. Finally

$$r = -\frac{2z_0}{\sqrt{\beta}} \ln\left(1 - \frac{z_0}{z_c}\right)\left(1 - \frac{z_0}{z_T}\right) + O(1) \quad (11)$$

Where β is a polynomial in $x = \left(\frac{z_0}{z_T}\right)^4$ and $y = \left(\frac{z_0}{z_c}\right)^2$ and is expressed as

$$\beta = -6 + 22x + 18y - 8y^2 - 34xy + 8xy^2 \quad (12)$$

The long distance behaviour (upper endpoint, $r \rightarrow \infty$) of the energy of the configuration can be expressed as

$$E = -\frac{ge^{\left(\frac{z_0}{z_c}\right)^2}}{\pi z_0 \sqrt{\beta}} \ln\left(1 - \frac{z_0}{z_c}\right)\left(1 - \frac{z_0}{z_T}\right) + O(1) \quad (13)$$

From, the long distance pseudo-potential turns out to be linear. The spatial string tension is given by

$$\sigma_s = \sigma \quad (14)$$

if $T \leq T_c$

$$\sigma_s = \sigma \frac{T^2}{T_c^2} \exp\left(\frac{T_c^2}{T}\right) - 1 \quad (15)$$

if $T \geq T_c$

where

$$T_c = \frac{1}{\pi} \sqrt{\frac{c}{2}} \quad (16)$$

This value of critical temperature corresponds to a point when $z_c = z_T$, that is the two walls coincide at the phase transition point and T_c turns out to be ≈ 210 MeV. Also it is found from and that

$$\frac{T_c}{\sqrt{\sigma}} = \sqrt{\frac{2}{e\pi g}} \quad (17)$$

Value of $g (\approx 0.94)$ comes from [29] the linear term of the Cornell potential. The approximation is in agreement with the lattice data for SU(3) gauge theory[23]. We have

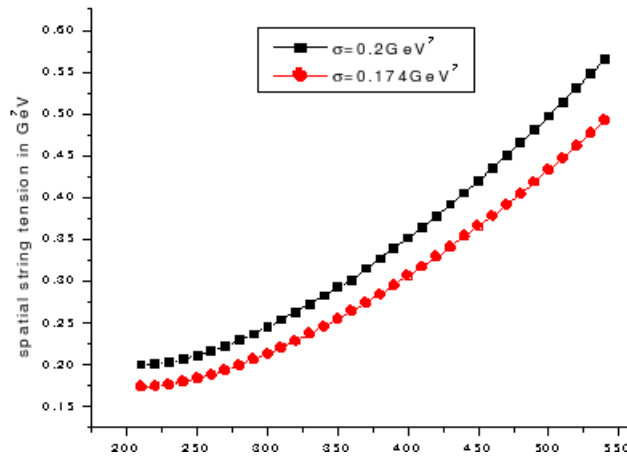


Fig. 3 Variation pattern of spatial string tension with temperature for upper and lower values of physical string tension.

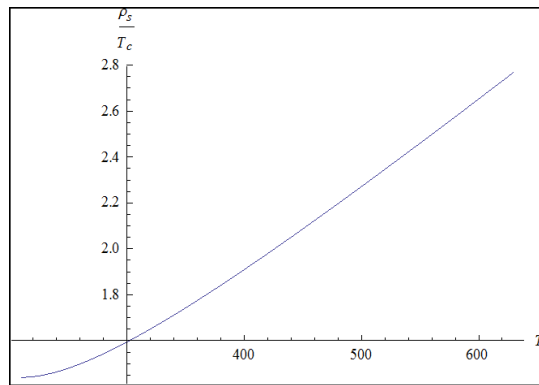


Fig. 4 Variation of ρ_s (in units of T_c) with temperature T (in MeV).

plotted (Figure3) the spatial string tension as a function of temperature for temperatures above critical temperature T_c . Data points have been plotted for the upper ($0.2GeV^2$) and lower limits ($0.87GeV^2$) of the physical string tension[30]. These limits may vary from one system (hadron configurations) to another, but our aim is to study the general behaviour, which should be same for all systems. The spatial string tension increases exponentially with temperature and the observed pattern shows similar behaviourism for the two different values of physical string tension, with the variation being slightly magnified as we proceed from the lower to the upper range.

When SU(2) gauge theory is considered and temperature dependence of spatial string tension is interrogated and it was found that

$$\frac{\sqrt{\sigma_s}}{T_c} = \frac{\rho_s}{T_c} = 1.44 \frac{T}{T_c} \exp\left[\frac{1}{2}\left(\frac{T_c}{T}\right)^2 - \frac{1}{2}\right] \tag{18}$$

(g depends on the number of colours, so its value has to be adjusted to SU(2) by employing fit $\frac{\sqrt{\sigma_s}}{T_c}$ at $T=T_c$ to the data from [31]).

The temperature dependence of string tension at high temperature is determined by the β function of gauge theory. Figure 4 demonstrates the variation of ρ_s/T_c with

temperature T for temperatures a few MeV above the critical temperature. For high temperatures, that is values greater than around 300 MeV, the plot shows a linear variation. An appreciable curvature is visible at lower values of T , that is near the critical temperature. Thus we can say the temperature dependence of string tension is very soft below T_c and sharp above T_c . Figure 3 and figure 4 evidently describe the extent of similarity between the $N_c=3$ and $N_c=2$ approach.

5. k-string Tensions under the Large N_c Formalism

There are many indications for a connection between QCD and the string theory, which has shown appearance in a broad domain of experimental phenomena and theoretical works [32]. Significant effort has been invested recently in QCD and pure Yang-Mills theories at large N in the studies of flux tubes induced by colour sources with an emphasis on its large N limit. Some mysterious features of the strong interactions become easily understandable, if our usual QCD with $N=3$ is 'close to' $SU(\infty)$ and if the latter theory is confining. $N=\infty$ theories are theoretically simpler, in particular there has been much progress in constructing weak coupling duals in string theory. Also, new stable confining strings appear at large N [15].

The naive QCD string is the flux tube that links heavy colour sources in the fundamental representation. It is referred to as the fundamental string and the string tension corresponding to it is called the fundamental string tension. However, the large N visualizations have found a novel realization in the studies of the spectrum of k -strings in the $SU(N)$ gauge theories. A k string is basically a flux tube generated between sources in the higher representation with non-vanishing N -ality. Consider the case when sources transform as $\Psi(x) \rightarrow z_k \Psi(x)$, under a global gauge transformation in the centre of the group, $z \in Z_N$ [33]. Gluon screening does in fact come into play. However, it cannot change k , but can change one source to another of the same k . The k string possesses the smallest string tension in the k class, and thereby it is a stable string. In other words, we can say that if a charge acquires a factor z_k , we shall refer to the string having N -ality k and the corresponding string tension will be denoted by σ_k . The fundamental string has N -ality $k=1$, and its string tension is denoted as σ_f or $\sigma_{k=1}$. In case of $SU(3)$, a $k=2$ string joining a diquark source to a distant antiquark source is the usual fundamental $k=1$ string over the entire separation. One has to step to at least $SU(4)$ for the possibility of a genuinely different $k=2$ string and $SU(6)$, for a $k=3$ string. Since gluons transform trivially under the centre, such a k string will not be screened down to a k' string, if $k' \neq k$. If, however $z_k = z_{k'}$ for all values of z , the k string can in fact transform into a k' string and then obviously $\sigma_k = \sigma_{k'}$.

Real QCD, according to definition, confines at intermediate and not at large distance scales because then the electric flux tubes would break and the static potential would go flat and the excited hadronic states with string like configurations would be metastable. For the intermediate distances, a linear potential is obtained. For this region itself, the string tensions agree qualitatively with both sine scaling and Casimir scaling[16]. Even

lattice simulations provide a substantial body of evidence that the string tensions in confining gauge obey scaling laws.

As already mentioned, there exists a linear potential between quarks for the fundamental and higher representations. The string tension then becomes representation dependent and roughly proportional to the eigen value of the quadratic Casimir operator of the representation. This proportionality of the potential to Casimir operator is called Casimir scaling. If σ_k is the string tension of the k string and σ_f is the string tension of the fundamental string, then Casimir formula is

$$\sigma_k = \frac{C_R}{C_{fund}} \sigma_f \quad (19)$$

where C_R is the quadratic Casimir coefficient for representation R defined as

$$T^a T^a = C_R I_R \quad (20)$$

and I is the unit matrix in the representation R , and T^a 's are the $SU(N)$ generators in the same representation. For large N , the Casimir formula expands [33] as

$$\sigma_k = k \left(1 - \frac{k}{N} + O(N^{-2}) \right) \sigma_f \quad (21)$$

From the above, it is clearly observed that the expansion runs in even as well as odd powers of $1/N$.

Recent studies in the super symmetric Y-M theories and M theory[34] suggest another possible scaling law called the sine scaling, in which the lowest string tension in each N -ality sector obeys

$$\frac{\sigma_k}{\sigma_f} = \frac{\sin\left(\frac{k\pi}{N}\right)}{\sin\left(\frac{\pi}{N}\right)} \quad (22)$$

At large N [33], the formula is expandable as follows

$$\sigma_k = k \left(1 - \frac{\pi^2}{6N^2} (k^2 - 1) + O(N^{-4}) \right) \sigma_f \quad (23)$$

Thus the large N expansion under the sine formula runs in even powers of $1/N$, whereas in Casimir formula all powers of $1/N$ are incorporated.

In the large N limit, the interactions between the flux tubes are suppressed in the powers of $1/N$ and therefore the lowest energy state of the system should be made of k fundamental flux tubes connecting the sources and hence

$$\frac{\sigma_k}{\sigma_f} \rightarrow k \quad (24)$$

, k fixed and $N \rightarrow \infty$ The constraint is satisfied by both Casimir scaling and the sine scaling formulae. Also, both these scaling formulae remain invariant under the replacement of k by $(N-k)$, i.e. exchange of quarks by antiquarks. Earlier calculations performed upon anisotropic lattice point out to the fact that the k string tensions lie midway between the sine scaling and Casimir scaling.

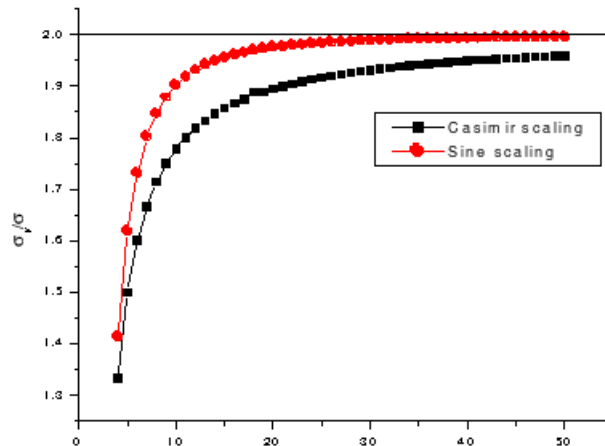


Fig. 5 Variation pattern of the ratio σ_k/σ with N_c for Casimir and sine scaling.

It is however worth noting that the corrections to large N behaviour occurs in the power series in $1/N^2$ rather than $1/N$ making the sine scaling much favourable and proximate to actual results. Figure 5 displays the variation of the ratio σ_k/σ with N_c for both the approaches, that is sine scaling as well as Casimir scaling. Both the curves demonstrate similar behaviourism with the sine scaling curve attaining slightly higher values as compared to the Casimir scaling curve. We have chosen $k=2$ strings for the entire plotted range ($N_c=3$ to $N_c=50$). Higher k strings can also be incorporated in the analysis but our aim is pinpoint the characteristic pattern which is similar for all higher k strings. At large values of N both the curves tend to approach the Casimir factor ($=2$). Thus we can say that as $N \rightarrow \infty$, the two approaches coherently reproduce similar behaviourism and this could substantially give boost to the validity of the effective emerging large N_c theory.

6. Glueball Dynamics and the String Tension

One of the main ingredients of the glueball dynamics is the adjoint string (or two fundamental strings)[35] occurring between the gluons in the two gluon glueballs. This adjoint string conjecture is inspired by the type two superconductor, which explores a new scenario of gluon-gluon interaction. Under this framework, the adjoint string is replaced by a pair of fundamental strings. The adjoint string is a natural extension of the fundamental string.

We are aware of the fact that the closed flux tube model of glueballs predict that the leading Regge Trajectory is essentially linear, with a slope value independent of N [35], that is

$$\alpha_{FT} = \frac{1}{8\pi\sigma} \quad (25)$$

for all values of N . However, when we consider the adjoint string model, it too predicts a linear Regge Trajectory

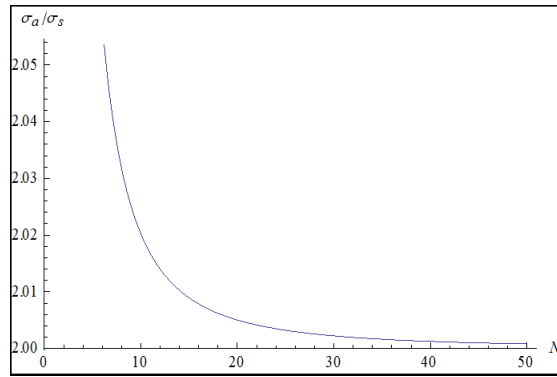


Fig. 6 Plot displaying the variation of the ratio σ_a/σ_s with the number of colours N When the spectrum of the glueballs is computed[37]

$$J = \frac{M^2}{2\pi\sigma_a} \quad (26)$$

where

$$M = 2 \int_0^{r_0} \frac{\sigma_a dr}{\sqrt{1-v^2(r)}} = \sigma_0 \pi r_0 \quad (27)$$

and

$$J = 2 \int_0^{r_0} \frac{\sigma_a r v(r) dr}{\sqrt{1-v^2(r)}} = \sigma_0 \frac{\pi}{2} r_0^2 \quad (28)$$

Here $2r_0$ is the length of the string joining the two gluons and acts as a rigid segment rotating with angular momentum J . The local velocity at a point along the segment is $v(r)=r/r_0$. The slope of the trajectory is

$$\alpha_{AS} = \frac{1}{2\pi\sigma_a} \quad (29)$$

and this evidently turns out to depend upon N , through the N dependence on σ_a/σ .

$$\frac{\sigma_a}{\sigma} = \frac{C_A}{C_F} = \frac{2N^2}{N^2 - 1} \quad (30)$$

Lattice calculations[36] as well as theoretical predictions support the fact that the dependence is close to Casimir scaling. Thus in the field theory σ_a is related to the string tension in the fundamental representation, σ . Figure 6 clearly demonstrates the dependence of N on string tension ratios. For the large N limit, the plot clearly depicts that the ratio approaches the Casimir scaling factor that is 2. The variation pattern projects out the fact that the $N_c=3$ limit is proximate to the ∞ limit and ratio is around 12.5 % higher for $N_c=3$.

$$M_n = 4\sqrt{\frac{n\sigma_a}{2}} \quad (31)$$

$n = 1, 3$

This equation is of particular interest because then the masses of the glueballs which otherwise depend upon σ_a can be connected to the fundamental string tension. The rotating glueballs lie entirely within a plane, therefore calculations in SU(3) gauge theory are identical to SU(2). The only prominent difference is that in SU(2) the adjoint string tension is $\sigma_a = \frac{8}{3}\sigma(SU(2))$, whereas for SU(3) its value is $\sigma_a = \frac{9}{4}\sigma(SU(2))$. These values of string tensions clearly demonstrate the fact that the SU(3) and the SU(2) gauge theories are clearly approximate to each other.

7. Relation of String Tension with the Mass of Hybrids and Gluelumps

We are well aware of the fact that gluons are colour octets and thereby are always confined. But this confinement property is never incorporated in the Standard Perturbation Theory (SPT), which is valid at short distances or regions of high momentum. It is however observed that beyond this region, the SPT displays unphysical singularities. Thus, the propagation of gluon in the confining vacuum is studied in the framework of the Background Perturbation Theory (BPT)[17], where non perturbative backgrounds contain confining co-relaters and the unphysical singularities of SPT are removed.

Several types of systems can substantially be formed by the confining gluons. They could possibly be glueball, hybrids and even gluelumps. It has been found empirically that the predicted spectrum[38] of these states have a very simple form and depends only upon the string tension σ_s and the strong coupling constant α_s . The analytic calculations of the spectrum are in good agreement with the lattice data.

The gluon exchange interaction between quark and antiquark occurs when the gluon is confined and is called the confined coulomb interaction. At small distances(less than 1GeV^{-1}), the confined potential corresponding to this interaction coincides with the standard Coulomb potential. Under this particular setting, the confined gluon is considered to be evolving in time together with static quark and antiquark, forming the gluon static hybrid. The mass of the hybrid (hybrid spectrum) is calculated in terms of the string tension. When the confined gluon acts as a propagator in the einbein path-integral representation and $\mu(t)$ is the einbein variable as in [39], the Green's function can be written as (for $T=T_0$)

$$G(x, y) = \int \frac{D\mu}{2\bar{\mu}} D\nu D\bar{\nu} e^{-\tau} G_3(R, T, \nu, \bar{\nu}, \mu) \quad (32)$$

Here two distinguishatory cases are considered

- 1) Large R and $R^2 \gg 1$ that is, large separation
- 2) Small R and $R^2 \ll 1$ that is, small separation

When the first case is considered, for the stationary point, the einbein parameter is found to be $\mu_0 = (\frac{\sigma}{R})^{\frac{1}{3}}$. Thereby, the mass of the hybrid at large R comes out to be

$$M_{hybrid}(R) = \sigma R + \frac{3}{2} \left(\frac{\sigma}{R}\right)^{\frac{1}{3}} + \frac{\sqrt{12}}{R} \quad (33)$$

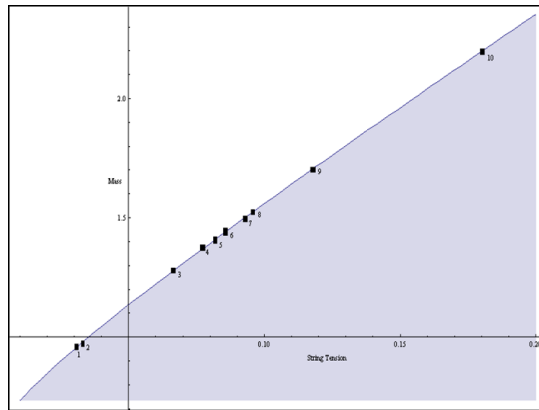


Fig. 7 Plot displaying the variation of the mass of the hybrids(in GeV) with respect to the string tension(in GeV^2) and the points depict the experimentally observed hybrid candidates: 1) $\eta'(958)$, 2) $a_0(980), f_0(980)$, 3) $f_2(1270)$, 4) $f_0(1370)$, 5) $\eta(1405)$, 6) $\eta(1440)$, 7) $f_0(1500)$, 8) $f_2'(1525)$, 9) $f_0(1710)$, 10) $f_2(2220)$.

The second factor on the RHS of the above equation corresponds to the characteristic $R^{-1/3}$ law for large R hybrid excitations[38]. The longitudinal and transversal excitations can be defined as

$$M_{hybrid}^{(long)} = \frac{3}{2^{n/s}} \left(\frac{\sigma}{R}\right)^{\frac{1}{3}} \left(n_z + \frac{1}{2}\right)^{\frac{2}{3}} \quad (34)$$

$$M_{hybrid}^{(trans)} = \frac{\sqrt{12}}{R} \left(\frac{\sigma}{R}\right)^{\frac{1}{3}} (n_{\perp} + \Lambda + 1) \quad (35)$$

where Λ corresponds to the angular momentum projection on the x-axis. The longitudinal excitation is new[38] whereas the transverse spectrum is quite close to the flux tube excitations. The observed spectrum is in coherence with the lattice calculations[40]. Thus, it becomes quite evident from the above equations that the hybrid particle mass is implicitly dependent upon the string tension parameter.

When we interrogated (Figure 7) the influence of string tension upon the hybrid mass a typical behavioural curve was observed. The points lying on curve exhibit the experimentally observed hybrid particles when the separation R is assigned the maximum value, which is 1GeV. The shaded area represents the region within which the hybrid particles would lie for lower R values. Thus, the entire spectrum of hybrid particles would be located within this region when the string tension ranges between 0.01 to $0.2GeV^2$. Since the exact dynamics of interior of the hybrid particles is unknown, we have chosen a wide range of the value of string tension. When the second case is considered, that is $\sigma R^2 \ll 1$, that is when $R \rightarrow 0$, for the stationary point $\mu = \mu_0$, the mass of the gluelump comes out to be

$$M_{gluelump} = 2\sqrt{3\sigma} \quad (36)$$

This value is in close agreement to the gluelump calculations performed in [41], where

$$M_0 = 2\left(\frac{a}{3}\right)^{\frac{3}{4}} (2\sigma_{adj})^{\frac{1}{2}} = 2\sqrt{3.096\sigma} \quad (37)$$

and $a(= 2.338)$ is the first zero of the Airy function. Thus, we can clearly observe that the string tension emerges out as the sole factor for determining the mass of the gluelumps. Table 1 depicts the values of string tensions calculated for various gluelump candidates.

Table 1 Table 1: String tensions in GeV^2 for Gluelump candidates

Gluelump candidate	◦ String tensions for data from ref[42]	★ String tensions for data from ref[42] coloumn 1	◦ String tensions for data from ref[43], column 1	★ String tensions for data from ref[43], column 2	◦ String tensions for data from ref ref[43], column 2	★ String tensions for data from ref ref[43], column 2
0++	0.3267	0.31657	————	————	————	————
1--	0.130208	0.126171	0.163147	0.158088	0.164174	0.159084
1+-	0.063075	0.0611192	0.081675	0.0791424	0.081675	0.0791424
1+	0.385208	0.373264	————	————	————	————
2--	0.175208	0.169776	0.219673	0.212862	0.220865	0.214017
2+-	0.2883	0.27936	0.359425	0.34828	0.347344	0.336574
3+-	0.2883	0.27936	0.359425	0.34828	0.356385	0.345335
3--	————	————	————	————	0.513195	0.497282
4--	0.378075	0.366352	0.472192	0.45755	0.491589	0.476346

◦ string tensions as evaluated from equation (36) ★ String tensions as evaluated from equation (37)

The values of string tensions lie within a range (0.06-0.51 GeV^2). It may however be pointed out that the upper limit of the string tension for gluelumps is far greater than average value for the hadrons. For the case of glueballs, the separation R reduces effectively which itself is the denominator factor in the string tension parameter and this eventually increases the string tension. Different data sets give approximately the same values of string tension for a particular glueball state. Thereby, we can say that the prospects are open for analyzing the possible experimental glueball candidates as viable theoretical background seems to be building up.

8. Regge Trajectory Phenomenology and String Tension

A linear potential between a quark and antiquark for mesons (quark and diquark for baryons) and the linearly rising Regge trajectory are immediate consequences of the string picture. The confinement potential at different length scales [44] is estimated by Cornell potential which is

$$V(R) \approx -\frac{4\alpha}{3R} + \sigma R \quad (38)$$

(where σ is the string tension) At long distances the second term is dominant which clearly corresponds to linear potential. The reproduction of linear potentials is one of the earliest

and most enthusiastic successes of the lattice gauge theory[45]. A linear relationship between J and M^2 ($M^2 = \alpha J + c$) is a clear manifestation of the strong forces between constituent quarks and directly corresponds to the fact that the strongly interacting particles (hadrons) are self generating and must lie on straight lines (Chew-Frautschi conjecture). The earliest postulation regarding the hadronic Regge trajectories was that they have a constant universal slope $\alpha = 0.93 \text{ GeV}^{-2}$ and this eventually led to the concept of universal string tension ($\sigma = 0.87 \text{ GeV/fm}$) since the slope parameter is directly related to string tension through the relation $\alpha = 1/(2\pi\sigma)$. Another method based upon the consideration of hadron size reproduces a constant value of string tension. For typical hadron mass of about 1 GeV and its radius as measured in electron scattering being 1 fm , the string tension comes out to be 1 GeV/fm . Earlier theoretical models on Regge phenomenology and even QCD utilized this particular value of string tension.

However, afterwards, the RT phenomenology was often attacked to investigate whether the RTs are actually straight lines in the entire energy interval or whether this is only valid asymptotically. An intrinsic connection is constantly being sought between the kinematics, type of potential and straight RT. The past few decades witnessed the proliferation of a large number of theoretical quark models [46], some of which clearly in favour of the linearity of RTs while the others claim non-linearity. Infact, some[46] even opted for the validity of partial linearism. Also, the availability of large amount of new data posed several challenges regarding the behaviour of linearity of the RTs. There by, these contradictions merely lead to a shear mix of confusions. At this stage the only rescue is the hadronic data which projects out the finest image of the hadronic world.

We analyzed the spectrum of hadrons[19] by the latest data available through the Particle Data Group[20], with the aim of pinpointing trajectories with which hadronic resonances can be associated. It was recognized that the entire range of Regge trajectories for hadrons are not straight and parallel lines. Out of total 66 plotted trajectories, 64.81% were essentially non-linear, 27.78% were essentially linear, while 7.41% were fairly linear. Thus, we can clearly say that the concept of universality of the slopes of hadrons and hence universal string tension indicates eventual violation. The essentially linear mesonic Regge trajectories have string tensions lying within a range, $0.02\text{-}0.111 \text{ GeV}^2$, whereas for the essentially linear baryonic Regge trajectories, the string tensions lie within the range $0.022\text{-}0.0455 \text{ GeV}^2$. Thus, on an average, the string tension for the baryons is less than for the mesons. In figure 8, we have plotted the string tension versus radial quantum number for some prominent essentially non-linear Regge trajectories. The black horizontal line displays the universal value of string tension. The plot clearly indicates substantial variation of the string tension from the universal value.

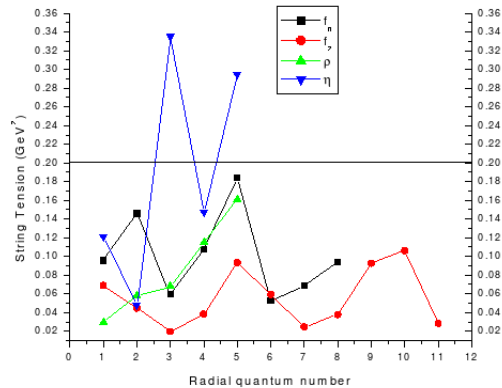


Fig. 8 Variation of string tensions with radial quantum number for the prominent f_0, f_2, η and ρ radial Regge Trajectories. The straight horizontal line denotes the standard universal value of string tension.

Conclusions

Our analysis evidently reveals the utility and importance of the string tension parameter in studying various prominent aspects related to QCD. The behavioural implications of the Wilson loops at high temperature helped in probing the deconfinement physics and thereby proved useful in determining the temperature dependence of the spatial string tension under the gluon chain model and also under the AdS/QCD picture. From these pictures, we can easily conclude that the temperature dependence of spatial string tension is very soft below the deconfinement temperature and sharp above it. The gluon chain model under the quenched $SU(N_c)$ clearly depicted that $N_c=3$ limit extensively stands apart from the $N_c=1$ limit. However, the appearance of new stable k-strings at large N_c helped in establishing the proximity of the $N_c=3$ limit to the large N_c limit.

String tension ratios for the large N_c limit were compared to Casimir scaling as well as the MQCD inspired conjectures. Both the approaches coincide for the large N_c limit. Study of glueball dynamics under the adjoint string model validates the scenario under which QCD incorporates strings apart from the fundamental string. The masses of hybrid particles and gluelumps are intrinsically dependent upon the string tension parameter and this connection helped us in relating the experimental data to the theoretical front. The string tension for gluelump candidates comes out to be larger than that for the hadronic particles.

The analysis of the string tension parameter under the Regge trajectory regime clearly indicated the violation of the orthodox notion of the concept universality of string tension. This is only plausible if the entire spectrum of hadronic RTs have same slope. However, the experimental data directly contradicted this notion. Thus, in the end we can conclude that the $N_c=2$ and the $N_c=3$ limits are quite close to each other, but they stand effectively apart from the $N_c=1$ limit. Also, our analysis clearly reveals the intimacy, connection

and similarity between the $N_c=3$ and the $N_c=\infty$ limit.

Acknowledgement

One of us (N.H.) gratefully acknowledges the R.F.S.M.S (Research Fellowship in Science for Meritorious Students) scheme of University Grants Commission, New Delhi for financial support.

References

- [1] T.Suzuki, Prog. Theor. Phys. 80, 929 (1988).
- [2] M.Baker, J.S.Ball and F.Zachariasen, Phys. Rev., D51, 1968 (1995).
- [3] S Mandelstam, Phys Rept., C23, 245(1976).
- [4] G.'t Hooft, Nucl.Phys. B, 190, 455 (1981).
- [5] T.Suzuki and I. Yotsuyanagi, Phys. Rev., D42, 425(1990).
- [6] K. G. Wilson, Phys. Rev., D10, 2445 (1974).
- [7] J. Adams et al. [STAR Collaboration], Nucl. Phys. A, 757, 102 (2005).
- [8] K. Adcox et al. [PHENIX Collaboration], Nucl. Phys. A, 757, 184(2005).
- [9] C. Borsis, Nucl. Phys.B, 261, 455 (1985)
- [10] C. Schmidt and T. Umeda, Nucl. Phys. A, 785, 274 (2007)
- [11] D. Antonov, S. Domdey and H.-J. Pirner, Nucl. Phys. A, 789, 357 (2007).
- [12] O. Andreev and V.I. Zakharov, Phys. Rev., D74, 025023(2006).
- [13] G. Bali, Phys. Rev., D62, 114503 (2000).
- [14] A. Armoni and M. Shifman, Nucl. Phys. B, 671, 67 (2003).
- [15] B. Lucini, M. Teper and U. Wenger, JHEP, 0406, 012 (2004).
- [16] J. Greensite and S. Olejnik, JHEP, 0209, 039 (2002).
- [17] G.'t Hooft, Nucl. Phys.B, 62, 444 (1973).
- [18] G.F.Chew and S.C.Frautschi, Phys.Rev.Letts. 8, 41 (1962)
- [19] S. Bisht, N. Hothi and G. Bhakuni, EJTP, 24, 299 (2010).
- [20] Particle Data Group, Review of Particle Physics-2008, Phys.Lett. B, 667, issues-1-5.
- [21] A. Nakamura and T. Saito, Prog. Theor. Phys., 115,189 (2006).
- [22] B. Svetitsky and L.G. Yaffe, Nuc. Phys. B, 120, 423 (1982).
- [23] F. Karsch, E. Laermann and M. Lutgemeier, Phys. Lett. B, 346, 94 (1995).
- [24] M. D'Elia, A. Di Giacomo and E. Meggiolaro, Phys. Rev., D67, 114504 (2003).
- [25] Y. Schroder and M. Laine, Proc. of Sci., 180, 37 (2005)

- [26] N. O. Agasian, Phys. Lett.B, 562, 257 (2003).
- [27] E. Braaten and A. Nieto, Phys. Rev., D51, 6990 (1995).
- [28] P. Petreczky and K. Petrov, Phys. Rev., D70, 054503 (2004)
- [29] O. Andreev, Phys. Rev., D73, 107901 (2006).
- [30] D. H. Perkins, Introduction to High Energy Physics, (Cambridge University Press, Cambridge, 2000) p45.
- [31] G. Bali, J. Fingberg, U.M. Heller, F. Karsch and K. Schilling, Phys. Rev. Lett., 71, 3050 (1993).
- [32] J. Polchinski, arXiv:hep-th/9210045.
- [33] M. Shifman, Acta Phys. Polon., B36, 3805 (2005).
- [34] D. Antonov and M.C. Diamantini, arXiv:hep-th/0406272v2
- [35] F. Bigazzi, A. L. Cotrone, L. Martucci and L. A. Pando Zayas, Phys. Rev., D71, 066002 (2005).
- [36] G. Bali, Nucl. Phys. Proc. Supp., 83, 422 (2000).
- [37] Yu. A. Simonov, Phys. Atom. Nucl., 70, 44 (2007).
- [38] Yu.S.Kalashnikova, D.S. Kuzmenko, Phys. Atom. Nucl., 64, 1716 (2001).
- [39] A. Yu. Dubin, A. B. Kaidalov and Yu.A.Simonov, Phys. Lett. B, 323, 41(1994).
- [40] K.J. Juge, J. Kuti and C. Moringstar, Nucl. Phys. Proc. Suppl., 73, 360 (1999).
- [41] Yu. A. Simonov, Nucl. Phys. B, 592, 350 (2001).
- [42] G. Bali and A. Pineda, Phys. Rev., D69, 094001(2004).
- [43] F. Buisseret, Eur. Phys. J., A38, 233 (2008).
- [44] E.Eichten, K.Gottfried, T.Kinoshita, K. D Lane., T. M. Yan., Phys. Rev., D17, 3090 (1978).
- [45] S. Kitahara, Y. Matsubara and T. Suzuki, Prog. Theor. Phys. 93, 1 (1995).
- [46] N. Hothi and S. Bisht, Indian J. Phy., 83, 339 (2009).